Rock and Soil Mechanics

Volume 43 | Issue 7 Article 4

9-20-2022

Rapid prediction method of soil-water characteristic curve of Yan'an compacted loess

Hai-man WANG

Wan-kui NI

Kui LIU

Rock and Soil Mechanics 2022 43(7): 1845−1853 ISSN 1000−7598
https: //doi.org/10.16285/j.rsm.2021.6696 rocksoilmech.researchcommons.org/journal

Rapid prediction method of soil-water characteristic curve of Yan'an compacted loess

WANG Hai-man[1], NI Wan-kui[1], LIU Kui[2]

1. College of Geology Engineering and Geomatics, Chang'an University, Xi'an, Shaanxi 710054, China
2. China Electronic Research Institute of Engineering Investigations and Design, Xi'an, Shaanxi 710000, China

Abstract: The traditional SWCC test method is time-consuming, and it is of great practical significance to develop a method that can quickly determine the SWCC of unsaturated soil. In order to predict the SWCC of compacted loess rapidly, the water potential and moisture content of compacted loess with different dry densities were tested, and the pore size distribution curve was measured using nuclear magnetic resonance (NMR) technology. Based on the test results, a rapid prediction method of the soil-water characteristic curve of Yan'an compacted loess was established based on the void ratio, and its accuracy was verified by the measured data. The results show that the fractal dimension D in the prediction model can be determined by the cumulative pore volume of two points (peak point and half-width point) on the pore size distribution curve and the slope of the pore size in a double logarithmic coordinate; and it can be expressed by the void ratio based on the linear relationship between void ratio and dominant pore diameter in logarithmic coordinates. The inlet value of SWCC is controlled by the diameter of macropore; the slope of the transition section is controlled by the volume of mesopore. There is a critical pore size in compacted loess, the residual water content is mainly controlled by the pore volume whose pore size is smaller than the critical pore size, and an empirical method is proposed to calculate the residual volume water content. Compared with traditional methods, the proposed method can save a lot of time in determining SWCC.

Keywords: compacted loess; unsaturated soil; nuclear magnetic resonance; soil-water characteristic curve; pore size distribution

1 Introduction

Soil-water characteristic curve (SWCC) plays a key role in unsaturated soil mechanics, and is widely used to predict the hydraulic conductivity, water storage and pollutant migration of unsaturated soil[1]. To date, many methods have been proposed to directly or indirectly determine SWCC of different types of soil. Among the direct measurement methods such as pressure plate instrument and tensiometer, the axis translation technology is usually used to measure the negative pore water pressure[2]. Indirect measurement methods are also widely used in engineering, including filter paper method and heat conduction method[3]. SWCC of unsaturated soil is measured under equilibrium conditions, then its measurement is usually time-consuming as a certain amount of time need to be spent for pore water stabilizing in soil at each matric suction stages. Though some scholars have proposed some indirect methods to quickly determine SWCC in recent years, it is still meaningful to develop an alternative method for determining SWCC of unsaturated soil[4−5].

SWCC is affected by many factors, which work via the pore structure change, resulting in the change of SWCC[6]. Frequently used soil-water characteristic curve models based on pore size distribution include Van Genuchten model[7] and Fredlund-Xing model[8], whose parameters are determined by fitting the measured data. SWCC also can be inferred directly from the pore size distribution curve, which is determined by MIP[9]. The pore volume measured by MIP is small as not all pores are inter connected[10]. Additionally, as the weathering product of rock, soil is more fragile than rock, and its internal structure is more complex. Since the soil structure can be partly damaged by MIP. Therefore, there will inevitably be some errors in determining SWCC based on the pore size distribution curve determined by MIP. Compared with MIP, NMR technology has more obvious advantages in determining the pore size distribution curve of soil as the NMR test process is fast and nondestructive. For this reason, NMR technology is widely used in soil pore size distribution measurement of indoor and field experiment[11−12].

NMR method has been widely used to determine soil water characteristics on the micro scale[5, 10, 13−14]. Bird et al.[10] explored the relative pore size distribution of saturated/unsaturated samples by stray field NMR technology. The micro drainage in the drying process is determined according to the measured relaxation time T_1. Tian et al.[13] revealed the mechanism of pore

Received: 9 October 2021 Revised: 28 March 2022
Tis work was supported by the National Natural Science Foundation of China (41931285) and Key R & D Projects in Shaanxi Province (2020SF-436).
First author: WANG Hai-man, male, born in 1993, PhD, PhD candidate, research interests: mechanics of unsaturated loess. E-mail: 1164727259@qq.com.
Corresponding author: NI Wan-kui, male, born in 1965, PhD, Professor, research interests: scientific research and teaching of loess mechanics. E-mail: niwankui@chd.edu.cn.

water migration in sand by using proton NMR setup. Chen et al.[5] fitted the measured T_2 curve with the pore size distribution function, and the key parameters of SWCC were obtained. Tao et al.[14] predicted the SWCC of Wuhan cohesive soil successfully by combining NMR technology with fractal model. Although NMR has been widely used to characterize the SWCC of soil, these methods depend on the fitting of pore size distribution curve, the mathematical models have not been developed for determining SWCC through basic physical parameters.

Based on the fractal model and NMR technology, a method is developed for quickly determining the soil-water characteristic curve of Yan'an loess in capillary state. And the important parameters in the fractal model are expressed by void ratio for improving the practicability of the model. In order to verify the reliability of the proposed method, the soil-water characteristic curve of soil is determined according to the proposed method, and then compared with the measured data by filter paper method. Since the void ratio measurement of soil is fast and simple, determining the SWCC of Yan'an compacted loess can save a lot of time by the proposed method.

2 Theory

2.1 NMR theory

Nuclear magnetic resonance (NMR) technology is a fast and nondestructive testing technology to explore the distribution of hydrogen proton content per unit volume. Because the pores of saturated samples have been filled with water completely, the pore distribution of loess can be indirectly tested by testing the distribution of hydrogen proton content. The T_2 curve, representing the pore size distribution curve, can be obtained by placing the saturated sample in the mini NMR analyzer PQ-001, which is developed by Suzhou Newmark company. The relationship between pore diameter d and T_2 can be expressed as[5, 15]:

$$d = 4T_2\rho_2 \tag{1}$$

where ρ_2 is the transverse surface relaxation (μm/ms). Since the NMR test was conducted in laboratory and completed in a short time, the temperature remained unchanged during the test in spite of the variation of ρ_2 with the soil mineral composition and temperature. Therefore, it is taken as a constant for a specific soil[16−17]. From Eq. (1), bigger T_2 value comes larger pore diameter. The NMR signal on the T_2 curve is directly proportional to the water content of the sample.

MIP and nitrogen adsorption method were used to solve the ρ_2 value by some scholars[18]. Schlumberger-Doll Research (SDR) equation, developed by Kenyon[19], is used to solve the surface relaxation ρ_2 owing to equipment limitations, which is

$$k_s = C\phi^4 T_{2LM}^2 \tag{2}$$

where k_s is the saturated permeability of soil; ϕ is the porosity; T_{2LM} is the logarithmic mean value of the T_2 distribution; and C is a constant.

The constant C in the SDR equation is proportional to the square of the surface relaxation[15, 20], namely $C = \rho_2^2$. Therefore, the follow equation can be derived:

$$k_s = \rho_2^2\phi^4 T_{2LM}^2 \tag{3}$$

Eq. (3) can also be written as

$$\rho_2 = \sqrt{\frac{k_s}{\phi^4 T_{2LM}^2}} \tag{4}$$

Porosity and permeability can be measured by the conventional tests. T_{2LM} can be determined by the statistics of T_2 distribution with SPSS software.

2.2 Fractal theory

According to the fractal theory of pore volume distribution, the relationship between the pore diameter and its corresponding number can be written as[21]

$$N = Cr^{-D} \tag{5}$$

where r is the pore radius; D is the fractal dimension of pore distribution; and N is the number of pores.

The pore volume V with pore radius less than r can be expressed as

$$V = \int_0^r \left(\frac{4\pi r^3}{3}\right) \mathrm{d}N = Ar^{3-D} \tag{6}$$

where $A = 4\pi CD/[3(D-3)]$.

In order to introduce the fractal model to SWCC, the following water content is expressed by volume water content. Therefore, the volume water content between r and $r + \mathrm{d}r$ from Eq. (6) is expressed as

$$\mathrm{d}(\theta - \theta_r) = \frac{4\pi r^3}{3}\mathrm{d}N \tag{7}$$

where θ is volume water content; and θ_r is the residual volume water content. According to Eq. (6) and Eq. (7), the effective saturation S_e is expressed as

$$S_e = \frac{\theta - \theta_r}{\theta_s - \theta_r} = \left(\frac{r}{R}\right)^{3-D} \tag{8}$$

where R is the maximum pore radius; and θ_s is the saturated volume water content.

With regard to the ideal capillary, the Young-Laplace equation can be used to describe the relationship between pore size and matric suction[22]:

$$\psi = \frac{4T_S \cos\alpha}{d} \tag{9}$$

where T_S is the surface tension on the water/air interface, T_S =72.75 kN/m as the temperature is 20 ºC [22]; α is the contact angle between soil particles and pore water, generally taken as 0°.

Substituting Eq. (9) into Eq. (8), the relationship between matric suction and volume water content can be derived as

$$\theta = \theta_r + (\theta_s - \theta_r)\left(\frac{R\psi}{2T_S \cos\alpha}\right)^{D-3} \tag{10}$$

The matric suction ψ is related to the pore diameter d from Eq. (9). According to the suction equilibrium theory, the water in the pores with pore diameter greater than d should be discharged completely under a certain matric suction condition. However, the water in some closed pores cannot be completely discharged actually[23] on a basic that the pores are non-ideal capillaries. Such problems also can be found in other methods for determining SWCC (such as pressure plate method). Therefore, the influence of incomplete drainage is not considered in the proposed method. The unknown parameters in Eq. (10) contains only residual water content, the maximum pore radius and fractal dimension. Once these parameters are obtained, the SWCC of soil can be calculated by Eq. (10).

3 Materials and methods

3.1 Materials

The loess in this study was collected from Yan'an new district. And the soil at the sampling point is Q_3 loess, whose basic physical parameters are shown in Table 1. The natural water content is about 11.9%, the maximum dry density is 1.69 Mg/m^3 by light compaction test, the optimum water content is 14.11%, the plastic limit is 16.1%, the liquid limit is 28.9%, and the plastic index I_P is 12.8. The particle size distribution is measured by the Bettersize2000 laser particle size analyzer, indicating that the loess sample is mainly composed of silt (about 78.99%), and the contents of sand and clay are roughly the same, with 10.39% and 10.62%, respectively (see Fig. 1).

Table 1 Basic physical parameters of test soil samples

Maximum dry density ρ_d /(Mg • m^{-3})	Optimum water content w /%	Specific gravity G_s	Liquid limit w_L /%	Plastic limit w_P /%	Sand content /%	Silt content /%	Clay content /%
1.69	14.11	2.72	28.9	16.1	10.39	78.99	10.62

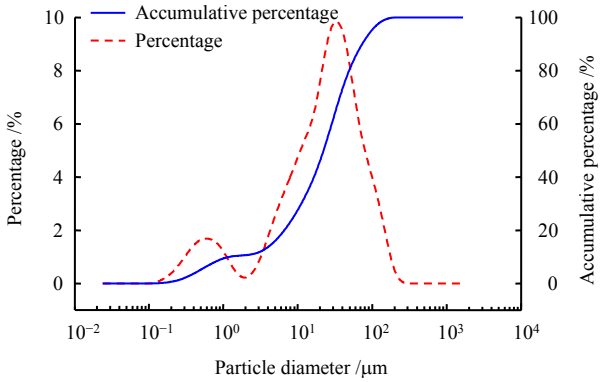

Fig. 1 Particle size distribution curves

3.2 Method

Twelve loess samples were compacted to the soil columns with water content of 10%, height of 20.0 mm, diameter of 79.8 mm, and dry densities of 1.45, 1.55, and 1.65 Mg/m^3, then the matric suction and NMR tests were conducted. There are 4 samples per dry density, and two samples with the same dry density are a group, a total of two groups. The same test procedure were performed as parallel test for the both groups of samples, and their mean value were taken to eliminate accidental errors. As the full range of matric suction can be measured by the filter paper method, it has the characteristics of wide measuring range, simple principle, low cost, and high accuracy, and the soil structure can not be damaged during the experiment, thus the filter paper method was selected to test the soil water characteristic curve of the sample. Double circle No.42 slow quantitative filter paper was used as the test filter paper in this test. A certain amount of distilled water was dropped on the surface of the sample evenly and slowly, and the sample water content increment shall not exceed 5%. Then the sample was sealed with a sealing bag and was put into the moisturizer for 3 days to make the water distribute evenly. The protective filter paper, test filter paper and protective filter paper were successively placed on the top of a sample that has been sealed for 3 days, and then another sample of the same group was placed on it, the two soil samples were compressed and fixed together with insulating tape. Finally, the soil samples were sealed with plastic film and sellotape, and were placed in a temperature and humidity control box at 30±2 ºC for 10 days. The water exchange between the soil sample and the filter

paper was completed and reached equilibrium after 10 days. Then the sealed samples were unwrapped, and the filter paper was weighed quickly. The matric suction can be calculated from the mass water content of the filter paper. After the suction test, the above steps were repeated to conduct humidification and suction test on the sample .

The nuclear magnetic resonance employed the mini NMR nuclear magnetic resonance analyzer PQ-001, which is developed by Suzhou Newmark company. The magnetic field strength of the permanent magnet of the NMR analyzer is 0.52 T (Tesla). In order to ensure the stability of the magnetic field, the temperature was maintained at 20±1 ℃. In order to eliminate the influence of hydrogen protons in the ring knife, all the ring knives used were teflon ring knives. The sample should be saturated for measuring complete pore size distribution curve, while it is difficult under normal atmosphere condition. Therefore, vacuum saturation was conducted as the water content reaches a certain value. Perforated stone and filter paper were place on the top and bottom of the sample to prevent the sample from being damaged during the saturation process. After the saturated samples were weighed, and then were placed in the NMR analyzer for NMR analysis. The free induction decay (FID) curve was measured by CPMG (CArr-Purcell-Meiboom-Gill) pulse sequence, in which the sampling repetition time is 100 ms. Finally, the FID curves of all samples were inverted (the inversion software based on the step-by-step iterative optimization algorithm provided by Suzhou Newmark company) to obtain the T_2 distribution data of each dry density sample, and then the T_2 distribution curves were drawn to determine the pore diameter distribution curve.

4 Methods and verification

4.1 Parameter solution

Using logarithms for Eq. (6) yields

$$\lg V = (3-D)\lg r + \lg A \tag{11}$$

Since the pore diameter d is twice the radius r ($d = 2r$), Eq. (11) can be expressed as

$$\lg V = (3-D)\lg d + \lg \frac{A}{2^{3-D}} \tag{12}$$

According to Eq. (12), if pore volume and pore diameter are the base-10 logarithms, respectively. And the slope of the scatter plot is k, then D=3−k.

The pore size distribution curve is required to solve the fractal dimension D, so the T_2 curve of NMR test (see Fig. 2 (a)) needs to be transformed into the pore size distribution curve. According to Eq. (1), the transverse surface relaxation ρ_2 should be solved firstly when the T_2 distribution curve was transformed into the pore size distribution. The transverse surface relaxation ρ_2 is related to the soil saturated permeability, porosity and the logarithmic mean value of T_2 distribution. For the sample with the dry density of 1.45 Mg/m^3, the saturated permeability k_s is 1.18×10^{-13} m^2, porosity ϕ is 0.49, geometric mean value of T_2 distribution T_{2LM} is 0.529 89 ms, and the obtained ρ_2 value is 2.69 μm/ms. With regard to the samples with the dry density of 1.55 Mg/m^3, the saturated permeability of the sample k_s is 6.14×10^{-14} m^2, porosity ϕ is 0.44, geometric mean value of T_2 distribution is 0.472 29 ms, and the obtained value of ρ_2 is 2.71 μm/ms. For the sample with the dry density of 1.65 Mg/m^3, and the saturated permeability k_s is 2.35×10^{-14} m^2, the porosity ϕ is 0.39, the geometric mean value of the T_2 distribution is 0.396 12 ms, and the obtained value of ρ_2 is 2.68 μm/ms. The ρ_2 of the same soil varies very little, which can be thought to be unchanged. The same result can be found in Tian et al.[16]. According to Eq.s (1) and (4), the T_2 distribution is transformed into the pore size distribution curve, and the pore volume of the soil per unit mass (1 g) is analyzed (see Fig. 2 (b)).

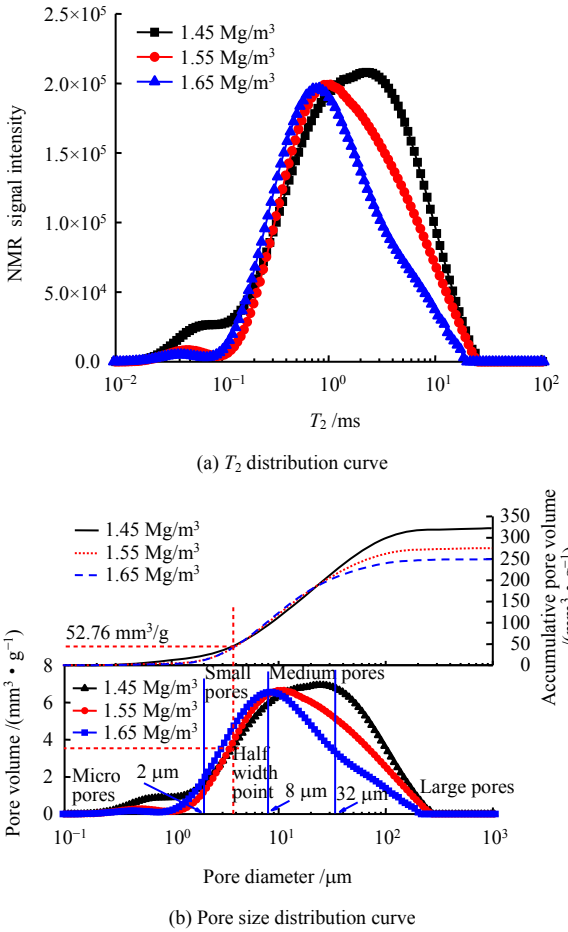

(a) T_2 distribution curve

(b) Pore size distribution curve

Fig. 2 NMR test and processing results

Young-Laplace equation (Eq. (9)), a key component of the proposed model, is derived from the force equilibrium at the air−water interface. It is applicable under certain pore size condition[24]. As capillary water may disappear, and adsorbed water is dominant in a low saturation state. Young-Laplace equation is no longer applicable in this case, and it is generally considered that this part corresponds to the residual water content. Therefore, the data of this part should be eliminated when the fractal dimension is solved[14]. There is a critical relaxation time T_{2r} in the T_2 curve, and the residual water content can be accurately predicted by using the water with a relaxation time less than T_{2r} [25]. According to Eq. (1), the critical relaxation time T_{2r} is proportional to the pore diameter, so there is a critical pore diameter d_r, and the pore volume with pore diameter less than d_r can accurately represent the residual volume water content. Half width point method is generally adopted for determining T_{2r}, that is, the value at 1/2 of the peak point on the T_2 curve is taken as T_{2r} [26]. Since Eq. (1) is used for converting T_2 to the pore diameter d on abscissa when the T_2 curve is converted into the pore diameter distribution curve, the half width point method can still be used to solve the critical pore diameter d_r in the pore diameter distribution curve (see Fig. 2), that is, the pore diameter at 1/2 of the highest point on the pore diameter distribution curve is taken as the critical pore diameter d_r, and the relationship between T_{2r} and d_r meets Eq. (1). The critical pore diameter d_r can be obtained as 3.8 μm (see Fig. 2 (b)). Therefore, the data with pore diameter less than 3.8 μm is discarded when calculating the fractal dimension.

The pore volume with pore diameter less than 3.8 μm corresponds to the residual water volume, so the critical pore diameter d_r of Yan'an compacted loess can be taken as 3.8 μm. The residual volume water content θ_r and residual mass water content w_r can be calculated by the following equations, respectively:

$$\theta_r = \theta_s \times \frac{V_r}{V_V} \tag{13}$$

$$w_r = \frac{\theta_r}{\rho_d} \tag{14}$$

where V_r is the pore volume with pore diameter less than d_r (mm^3/g), which is taken as 52.76 mm^3/g in this paper (see Fig. 2); V_V is the total pore volume (mm^3/g); and ρ_d is the dry density (Mg/m^3).

The residual volume water contents of compacted loess with dry density of 1.45, 1.55 and 1.65 Mg/m^3 are 7.9%, 8.5% and 8.6%, respectively; and the corresponding mass residual water content are 5.4%, 5.5% and 5.2%, respectively. The residual volume water content slightly increases with the increase of dry density[27]. The mass bound water content of Q_3 loess is measured to be 5.8% by Hou et al.[28] using isothermal adsorption method, which is very close to the measured value by NMR technology in this paper, proving the rationality of 3.8 μm for the critical pore diameter d_r of Yan'an compacted loess.

Sorting the data that conforms to the fractal model, and a scatter diagram is drawn with lg$d$ as the abscissa and lg$V$ as the ordinate (see Fig. 3). The data present obvious linear relationship, and are linear fitted, that is $y = kx + b$. The fitting expression and parameters are shown in Table 2, where R^2 is the fitting correlation coefficient.

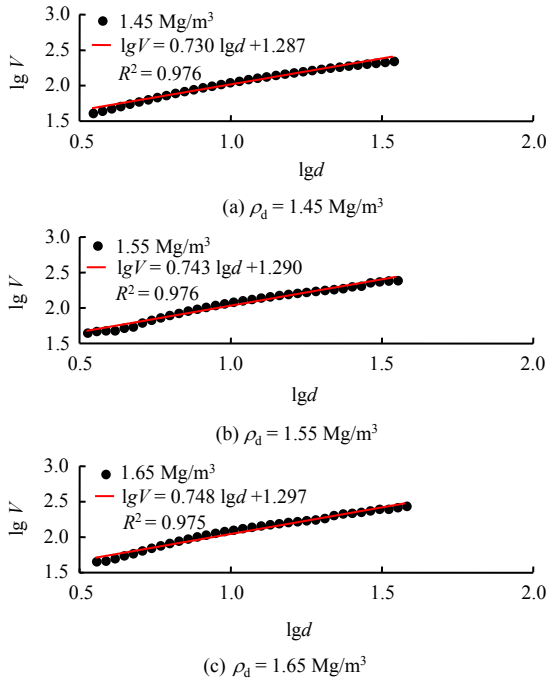

Fig. 3 Calculation of fractal dimension

Table 2 Linear fitting results

Dry density /(Mg • m^{-3})	Slope k	b	R^2	D
1.45	0.730	1.287	0.976	2.270
1.55	0.740	1.290	0.976	2.266
1.65	0.748	1.297	0.975	2.252

Table 2 shows that the fitting correlation coefficients of samples with different dry densities are greater than 0.97 with good fitting effect. The maximum pore diameter $2R$ is the pore diameter when the cumulative pore volume on the cumulative pore diameter distribution curve no longer increases. According to the definition

of maximum pore diameter and the data in Fig. 3, the maximum pore radius R of compacted loess with dry density of 1.45, 1.55 and 1.65 Mg/m^3 are 138, 128 and 100 μm respectively. At this time, the maximum pore radius, fractal dimension and residual volume water content have been obtained from NMR data, and the soil water characteristic curve of Yan'an compacted loess can be calculated by Eq. (10).

4.2 Parameter optimization

Although the soil water characteristic curve of samples can be predicted by the above method to measure the pore size distribution curve of samples with different dry densities using NMR technology, it is difficult to measure the pore size distribution curve of each dry density sample in practical application. Therefore, the above parameters should be optimized, and the parameters in the model (fractal dimension, volume residual water content and maximum pore diameter) should be expressed by basic physical indicators.

The pore volume first increases and then decreases with the increase of pore size. The pore at the peak point is the most abundant in the sample, so the pore at the peak point is defined as the dominant pore, and the corresponding pore diameter is the dominant pore diameter. The dominant pore diameter d_a of the sample moves to the left with the increase of dry density, that is, d_a decreases with the decrease of pore ratio e[29]. For example, d_a reduces from 24 μm to 8.7 μm when the dry density of the sample increases from 1.45 Mg/m^3 to 1.65 Mg/m^3(see Fig. 2). The relationship curve between e and d_a is drawn in logarithmic coordinates (see Fig. 4), and it obviously shows that e and d_a are linear. Phadnih et al.[30] also found the same rule, and theoretically deduced the linear relationship between e and d_a. The results of Wang et al.[31] are also shown in Fig. 4 for comparison. The slope of e and d_a linear relationship seems to be fixed, but the intercept is different, which may vary with soil.

Li et al.[32] assumed that the pore size distribution curve conforms to the normal distribution in the semi logarithmic coordinate, predicted the pore diameter distribution curve, good results were achieved. According to the characteristics of normal distribution, the cumulative pore volume of the dominant pore diameter d_a at the peak point is $e/(2G_s)$. Combining Fig. 4 and the properties of normal distribution, the dominant pore diameter and the corresponding cumulative pore volume can be calculated with the known void ratio e. Li et al.[33] proposed that the pore volume of small pores varies little with dry density, which is similar to the results of this study (see Fig. 2). The pore diameter of half width point is 3.8 μm, and the pore volume smaller than its pore diameter does not change with dry density. The pore volume with pore diameter smaller than 3.8 μm is calculated to be 52.76 mm^3/g. According to the above two points (peak point and half width point), a straight line of d and V can be determined in logarithmic coordinate. Since these two points are on the straight line in Fig. 3, the slope k can be expressed as

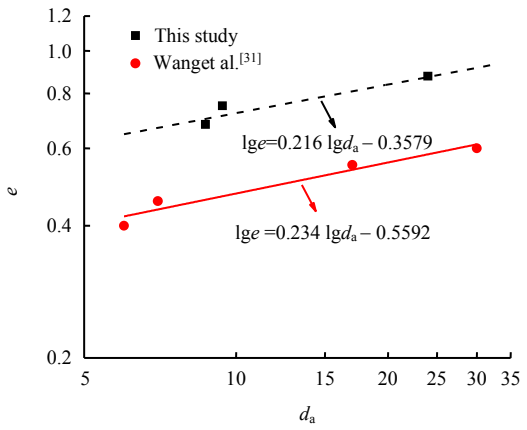

Fig. 4 Relationship between e and d_a

$$k = 0.216 \cdot \frac{\lg \dfrac{e}{2G_s} - \lg 52.76}{\lg e + 0.357\ 9 - 0.216 \lg 3.8} \tag{15}$$

Then the fractal dimension D can be written as

$$D = 3 - 0.216 \cdot \frac{\lg \dfrac{e}{2G_s} - \lg 52.76}{\lg e + 0.357\ 9 - 0.216 \lg 3.8} \tag{16}$$

Because the residual volume of samples with different dry densities is 52.76 mm^3/g, the residual volume water content can be expressed as

$$\theta_r = \frac{52.76 G_s}{1\ 000(1+e)} \tag{17}$$

According to the nature of normal distribution, the maximum pore diameter in semi logarithmic coordinate is twice the dominant pore diameter, which can be expressed as

$$\lg(2R) = 2 \lg d_a \tag{18}$$

That is

$$2R = 10^{\frac{2(\lg e + 0.357\ 9)}{0.216}} \tag{19}$$

Thus all parameters in Eq. (10) are expressed by void ratio, and the soil−water characteristic curve of Yan'an Q_3 loess can be determined with known void ratio.

4.3 Method validation

The parameters D, θ_r, and R, obtained from the above method, are used to determine the SWCC of all tested samples with different dry densities. The obtained SWCC is compared with the measured data in Fig. 5. It can be seen that the predicted curve is in good agreement with the measured data.

There are some differences between the predicted curves and the measured data. The reasons for this difference are as follows: (1) The pore shape is assumed to be fixed, while may vary in the actual situation. (2) The influence of adsorbed water is ignored as capillary theory and Young-Laplace equation are applied in the proposed model. (3) The pore water larger than its corresponding pore diameter is assumed to be completely discharged under a certain suction condition, the influence of closed pores is ignored. The prediction accuracy gradually decreases with the increase of dry density, its reason is that the loess sample is in the unsaturated state during SWCC test, while in the saturated state during NMR test. In the process of saturation, on the one hand, the dissolution of soluble salt causes the connection or expansion of pores; on the other hand, the combined water film between soil particles thickens and the soil skeleton expands due to the entry of water, and this phenomenon becomes more obvious with the increase of dry density[34]. The change of SWCC is reflected by the influence of soil pore condition, so the accuracy of SWCC prediction based on NMR curve will decrease with the increase of dry density. Moreover, since Young-Laplace equation is an important part of the model, the application of the proposed method should be limited to Yan'an compacted loess with medium to high saturation, that is, the capillary effect of pore water is dominant in the capillary state. Other methods should be adopted for fine-grained soil with large amount of adsorbed water.

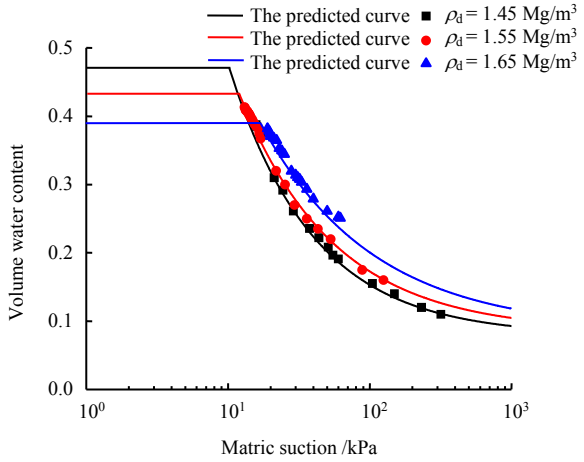

Fig. 5 Comparison of the predicted and measured SWCC data

Figure 5 clearly illustrates that the saturated volume water content decreases, and the soil water characteristic curve of the sample gradually slows down with the increase of dry density. Additionally, the air entry value also increases to a certain extent[35]. However, the residual water contents of soil water characteristic curve of samples with different dry densities are very close. The main factors affecting the soil water characteristic curve are soil mineral composition, pore structure, soil shrinkage and stress history. The water loss state of soil and the corresponding matric suction only depend on the number and diameter of pores for the same kind of soil, so the soil water characteristic curve indirectly reflects the pore size distribution of soil. The SWCC evolution mechanism will be analyzed in terms of pore volume below.

4.4 SWCC evolution mechanism

The pore size distribution curve in Fig. 2 can be divided into four types: micro pores ($d \leqslant 2$ μm), small pores (2 μm< $d \leqslant 8$ μm), medium pores (8 μm< $d \leqslant$ 32 μm) and large pores (d >32 μm)[36]. The volume of various pores in the pore size distribution curve is counted to obtain the histogram of various pore volumes of samples with different dry densities (see Fig. 6).

Low density soil samples have many large pores, which can store a large amount of water in saturated state, and have high saturated water content. The pore volume of the sample gradually decreases, and the maximum pore diameter and dominant pore diameter decrease with the increase of dry density (see Fig. 2). The volume and diameter of large pores in the soil decrease with the increase of the initial dry density of the sample, resulting in the increase of matric suction. Therefore, the pressure (air entry value) required for air entering the soil pores also increases. The slope of SWCC reflects the change rate of volume water content with matric suction. The larger the slope is, the faster the volume water content changes with the matric suction, and the faster the water loss rate of the soil is. With the increase of dry density, the medium pores volume (dominant pores) gradually decreases, making the water loss rate of soil slow down. Therefore, the slope of SWCC gradually decreases with the increase of dry density. The gradual increase of the dry density of the sample can be regarded as a compression process. The volume of large pores and medium pores of samples with different dry densities decrease with the increase of dry density, while the volume of small pores increases, indicating that the compression of large pores and medium pores will produce small pores in the compression process. The volume of micro

pores does not mainly change with dry density. According to the capillarity theory, the water in the large pores is discharged firstly in the water loss process of soil, and then the water in the small pores. Therefore, the residual water content should be closely related to the water in the micro pores. The residual water content also varies little due to slightly volume change of micro pores.

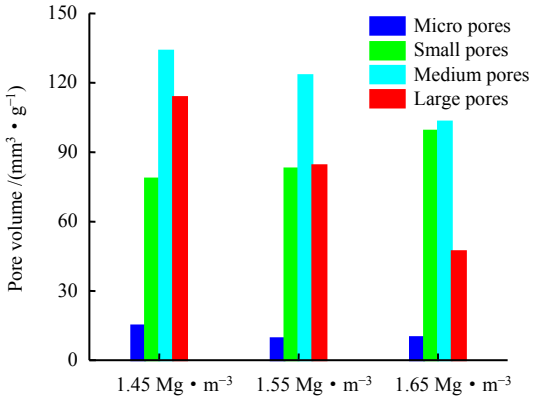

Fig. 6 Statistics of different types of pore volumes

5 Conclusions

(1) The void ratio and dominant pore diameter have a linear relationship in the double logarithmic coordinate, and the slope of soil in different regions is essentially the same, while the intercept is different. Fractal dimension D can be expressed by void ratio (see Eq. (16)).

(2) There is a critical pore diameter (d_r=3.8 μm) in Yan'an compacted loess, and an empirical method for calculating the critical pore diameter is proposed. The volume residual water content of soil can be predicted by the pore volume with pore diameter less than d_r approximately.

(3) Considering the long test cycle of SWCC test, the NMR technology and pore fractal model are combined to achieve the purpose of rapid and accurate prediction of SWCC of loess.

(4) The air entry value of SWCC is controlled by the diameter of large pores. The smaller the diameter of large pores is, the larger the air entry value is. The slope of the transition section is controlled by the medium pores volume. The larger the medium pores volume is, the larger the slope of the transition section is, indicating the water loss faster. The residual volume water content of samples with different dry densities is essentially the same.

References

[1] CHEN P, WEI C, MA T. Analytical model of soil-water characteristics considering the effect of air entrapment[J]. International Journal of Geomechanics, 2015, 15(6): 04014102.

[2] LU N, WAYLLACE A, CARRERA J, et al. Constant flow method for concurrently measuring soil-water characteristic curve and hydraulic conductivity function[J]. Geotechnical Testing Journal, 2006, 29(3): 230−241.

[3] AGUS S S, SCHANZ T. Comparison of four methods for measuring total suction[J]. Vadose Zone Journal, 2005, 4(4): 1087−1095.

[4] WAYLLACE A, LU N. A Transient water release and imbibitions method for rapidly measuring wetting and drying soil water retention and hydraulic conductivity functions[J]. Geotechnical Testing Journal, 2012, 35(1): 103−117.

[5] CHEN P, LIU J, WEI C, et al. Approach to rapidly determining the water retention curves for fine-grained soils in capillary regime based on the NMR technique[J]. Journal of Engineering Mechanics, 2017, 143(7): 4017032.

[6] BECKETT C T S, AUGARDE C E. Prediction of soil water retention properties using pore-size distribution and porosity[J]. Canadian Geotechnical Journal, 2013, 50(4): 435−450.

[7] VAN GENUCHTEN M T. A Closed-form equation for predicting the hydraulic conductivity of unsaturated soils[J]. Soil Science Society of America Journal, 1980, 44(5): 892−898.

[8] FREDLUND D G, XING A. Equations for the soil-water characteristic curve[J]. Canadian Geotechnical Journal, 1994, 31(4): 521−532.

[9] SIMMS P H, YANFUL E K. Predicting soil-water characteristic curves of compacted plastic soils from measured pore-size distributions[J]. Géotechnique, 2002, 52(4): 269−278.

[10] BIRD N R A, PRESTON A R, RANDALL E W, et al. Measurement of the size distribution of water-filled pores at different matric potentials by stray field nuclear magnetic resonance[J]. European Journal of Soil Science, 2005, 56(1): 135−143.

[11] DUSCHL M, GALVOSAS P, BROX T I, et al. In situ determination of surface relativities for unconsolidated sediments[J]. Water Resources Research, 2015, 51(8): 6549−6563.

[12] TYROLOGOU P, DUDENEY A W L, GRATTONI C A. Evolution of porosity in geotechnical composites[J]. Magnetic Resonance Imaging, 2005, 23(6): 765−768.

[13] TIAN H, WEI C, WEI H, et al. An NMR-based analysis of soil-water characteristics[J]. Applied Magnetic Resonance, 2014, 45(1): 49−61.

[14] TAO Gao-liang, CHEN Yin, YUAN Bo, et al. Predicting soil-water retention curve based on NMR technology and fractal theory[J]. Chinese Journal of Geotechnical Engineering, 2018, 40(8): 1466−1472.

[15] KONG L, SAYEM H M, TIAN H. Influence of drying-wetting cycles on soil-water characteristic curve of undisturbed granite residual soils and microstructure mechanism by nuclear magnetic resonance (NMR) spin-spin relaxation time (T-2) relaxometry[J]. Canadian Geotechnical Journal, 2018, 55(2): 208−216.

[16] TIAN Hui-hui, WEI Chang-fu. A NMR-BASED testing and analysis of adsorbed water content[J]. Scientia Sinica (Technologica), 2014, 44(3): 295−305.

[17] GODEFROY S, KORB J P, FLEURY M, et al. Surface nuclear magnetic relaxation and dynamics of water and oil in macroporous media[J]. Physical Review E, 2001, 64(2): 21605.

[18] YAO Y, LIU D. Comparison of low-field NMR and mercury intrusion porosimetry in characterizing pore size distributions of coals[J]. Fuel, 2012, 95: 152-158.

[19] KENYON W E. Nuclear magnetic resonance as a petrophysical measurement[J]. Nuclear Geophysics, 1992, 6(2): 153−171.

[20] KLEINBERG R L, FLAUM C, GRIFFIN D D, et al. Deep sea NMR: methane hydrate growth habit in porous media and its relationship to hydraulic permeability, deposit accumulation, and submarine slope stability[J]. Journal of Geophysical Research: Solid Earth, 2003, 108(B10): 2508.

[21] PFEIFER P, AVNIR D. Chemistry in noninteger dimensions between two and three. I. Fractal theory of heterogeneous surfaces[J]. Journal of Chemical Physics, 1984, 80(7): 3558−3565.

[22] LU N, LIKOS W J. Unsaturated soil mechanics[M]. New York: Wiley, 2004.

[23] CHEN P, WEI C, MA T. Analytical model of soil-water characteristics considering the effect of air entrapment[J]. International Journal of Geomechanics, 2015, 15(6): 4014102.

[24] LU N, KHORSHIDI M. Mechanisms for soil-water retention and hysteresis at high suction range[J]. Journal of Geotechnical and Geoenvironmental Engineering, 2015, 141(8): 4015032.

[25] TAO Gao-liang, LI Jin, ZHUANG Xin-shan, et al. Determination of the residual water content of SWCC based on the soil moisture evaporation properties and micro pore characteristics[J]. Rock and Soil Mechanics, 2018, 39(4): 1256−1262.

[26] ZHANG Shi-min, SUN Yin-suo, ZHANG Li-sha, et al. Application of nuclear magnetic resonance technology in pore analysis of unfrozen soil[J]. Yangtze River, 2019, 50(11): 183−188.

[27] LIU Feng-yin, ZHANG Zhao, ZHOU Dong, et al. Effects of initial density and drying-wetting cycle on soil water characteristic curve of unsaturated loess[J]. Rock and Soil Mechanics, 2011, 32(Suppl. 2): 132−136.

[28] HOU Xiao-kun, LI Tong-lu, XIE Xiao, et al. Effect of undisturbed Q3 loess's microstructure on its SWCC[J]. Journal of Hydraulic Engineering, 2016, 47(10): 1307−1314.

[29] LI Yan, LI Tong-lu, HOU Xiao-kun, et al. Prediction of unsaturated permeability curve of compaction loess with pore-size distribution curve and its application scope[J]. Rock and Soil Mechanics, 2021, 42(9): 2395−2404.

[30] PHADNIS H S, SANTAMARINA J C. Bacteria in sediments: pore size effects[J]. Géotechnique Letters, 2011, 1(4): 91−93.

[31] WANG J, LI P, MA Y, et al. Evolution of pore-size distribution of intact loess and remolded loess due to consolidation[J]. Journal of Soils and Sediments, 2019, 19(3): 1226−1238.

[32] LI P, SHAO S, VANAPALLI S K. Characterizing and modeling the pore-size distribution evolution of a compacted loess during consolidation and shearing[J]. Journal of Soils and Sediments, 2020, 20(7): 2855−2867.

[33] LI Hua, LI Tong-lu, ZHANG Ya-guo, et al. Relationship between unsaturated permeability curve and pore-size distribution of compacted loess with different dry density[J]. Journal of Hydraulic Engineering, 2020, 51(8): 979−986.

[34] ZHAO Tian-yu, WANG Jin-fang. Soil-water characteristic curve for unsaturated loess soil considering density and wetting-drying cycle effects[J]. Journal of Central South University (Science and Technology), 2012, 43(6): 2445−2453.

[35] GALLAGE C P K, UCHIMURA T. Effects of dry density and grain size distribution on soil-water characteristic curves of sandy soils[J]. Soils and Foundations, 2010, 50(1): 161−172.

[36] LEI X. The types of loess pores in china and their relationship with collapsibility[J]. Science in China, Ser.B. 1988(11): 1398−1411.